Article:

Grisaro, H.Y., Edri, I.E. and Rigby, S.E. orcid.org/0000-0001-6844-3797 (2021) TNT equivalency analysis of specific impulse distribution from close-in detonations. International Journal of Protective Structures, 12 (3). pp. 315-330. ISSN 2041-4196

https://doi.org/10.1177/2041419620972423

TNT equivalency analysis of specific impulse distribution from close-in detonations

Hezi Y. Grisaro[a,1], Idan E. Edri[a], Samuel E. Rigby[b]

[a] Faculty of Civil & Environmental Engineering, National Building Research Institute, Technion - Israel Institute of Technology, Haifa, Israel

[b] Department of Civil & Structural Engineering, University of Sheffield, Mappin Street, Sheffield, S1 3JD, UK

Abstract

Detonation of a high explosive close to a structural component results in a blast load that is highly localized and nonuninform in nature. Prediction of structural response and damage due to such loads requires a detailed understanding of both the magnitude and distribution of the load, which in turn are a function of the properties and dimensions of the structure, the standoff from the charge to the structure, and the composition of the explosive. It is common to express an explosive as an equivalent mass of TNT to facilitate the use of existing and well-established semi-empirical methods. This requires calculation of a TNT equivalency factor (EF), i.e. the mass ratio between the equivalent mass of TNT and the explosive mass in question , such that a chosen blast parameter will be the same for the same set of input conditions aside from explosive type. In this paper, we derive EF for three common explosives: C4, COMP-B, and ANFO, using an equivalent upper bound kinetic energy approach. A series of numerical simulations are performed, and the resultant magnitudes and distributions of specific impulse are used to derive the theoretical upper bound kinetic energy that would be imparted to a flexible target. Based on the equivalent mass of TNT of each explosive, which is required to impart the same kinetic energy for a given target size and standoff distance as of TNT, the EF is calculated. It is shown that in the near-field, the EFs are non-constant and are dependent on both standoff and target size. The results in the current study are presented in a scaled form and can be used for any practical combination of charge mass, distance from the charge to the target, target size, thickness, and density.

Keywords: TNT equivalency, Blast, Energy equivalent impulse, Near-field, Numerical analysis

[1] Corresponding author, e-mail: hezi@technion.ac.il

1. Introduction

The prediction of the blast wave parameters following detonation of a high explosive is important for the assessment of the dynamic response of a structure subjected to that load. The blast wave parameters, such as the peak overpressure and impulse, and the magnitude and distribution over the structural element significantly affect its dynamic response. Analytical methods for the prediction of the blast parameters are rarely available, and therefore, there are three main approaches for their evaluation, as follows:

I. Empirical (or semi-empirical) models, which are given in the form of equations or diagrams. Examples are the methods given in design manuals, such as the UFC 3-340-02 (USACE, 2008), or the commonly used equations given by (Kingery and Bulmash, 1984). Being such fast running tools, these models are preferred by engineers, although they are limited to geometrically simple scenarios and charge configurations.

II. Numerical simulations using hydro-codes (e.g. Grisaro and Edri, 2017; Shin et al., 2015). Although this approach is expensive in terms of computational time and resources, it provides more accurate results for complex geometries, various charge shapes, and close-in detonations.

III. Experimental studies for more specific and special cases (e.g. Codina and Ambrosini, 2018; Rigby et al., 2019a).

A structure that is exposed to a close-in detonation is expected to experience high magnitudes of overpressure and impulse. A close-in detonation is commonly defined for scaled distances that are lower than 1.2 m/kg$^{1/3}$ (ASCE, 2011; CSA, 2012; Ritchie et al., 2018). In addition to the high pressure and impulse magnitudes in the near-field regime, the blast load in such conditions is expected to be nonuniform over the loaded face of the structure. These aspects make the prediction of the blast load parameters nontrivial and challenging, especially by using simplified methods. Although such methods are very common due to their low computational cost, their accuracy in the near-field regime is doubtful. Furthermore, while empirical models consider an idealized spherical or hemispherical charge shapes, the charge shape may be different, and in the near-field regime, the shape may significantly affect the overpressure environment around the charge (Adhikary et al., 2017; Sherkar et al., 2014). Thus, the two other methods are frequently used. When experimental work is not possible or practical, i.e. when a large number of scenarios is of interest, numerical simulations may naturally be the preferable option.

Many of the above semi-empirical approaches assume the explosive is formed of TNT. However, when a different explosive is used, for the same charge mass, different blast parameters, such as the peak overpressure and impulse, are derived (Cooper, 1996; Esparza, 1986). In such cases, an equivalent charge mass of TNT is defined, which would yield the same blast load parameter (impulse, overpressure, etc.) at the same distance. The mass ratio of the equivalent TNT charge mass and the examined explosive mass is defined as the TNT equivalency factor (EF). Available methods (Grisaro and Edri, 2017) for predicting the EF values consider several parameters such as the internal charge energy, detonation velocity, Chapman-Jouguet pressure, and explosive density. In a previous study (Grisaro and Edri, 2017), it was found that for the far-field regime (for $3 \leq Z \leq 40$ m/kg$^{1/3}$), both the EFs for impulse and overpressure strongly depend on the energy ratio of the examined explosive and TNT. However, a different function of the energy ratio was found for the impulse and the peak overpressure. Also, it was found that a constant value of EF can be used for impulse and pressure for the entire range of scaled distances referring to the far-field regime. However, there are currently very few studies on TNT equivalency in the near-field regime. These studies show that unlike the far-field regime, in the near-field regime a unique EF value for a specific blast parameter cannot represent the real behavior (e.g. Xiao et al., 2020, 2019). Therefore, in addition to affecting the impulse and pressure values, the EF in the near-field may affect also the *spatial distribution* of the blast load over the structural element.

The response of thin plates subjected to close-in detonations was studied by (Rigby et al., 2019a), using a combination of experimental, numerical, and analytical tools. Since the blast load duration in a close-in detonation event is expected to be short compared to the period of vibration of the structure, the dominant load parameter is the impulse. The impulse distribution is expected to be nonuniform, as shown in Figure 1a. Thus, (Rigby et al., 2019a) defined an impulse enhancement factor, which enables a complex distributed load to be expressed as an equivalent uniform load which would impart the same kinetic energy to a target plate. It was shown that peak displacement was closely correlated to energy equivalent impulse, and weakly correlated to total impulse, therefore the peak displacement could be better predicted with knowledge of the distribution of loading, as well as its magnitude.

Assuming that a plate is subjected to nonuniform impulsive loading, the following cases are possible. Firstly, under the assumption that the deformation modes possess infinite resistance to shear as shown in Figure 1b, the entire plate acts as a rigid body and the deformation mode represents a lower bound of the kinetic energy. A second possible extreme scenario includes a deformation mode in which the shear resistance between two mass particles of the plate is zero. Therefore, in this case, the kinetic energy is characterized by its upper bound. It was also shown by (Rigby et al., 2019a) that two different targets, each experiencing a load that imparts the same upper bound kinetic energy, will experience similar dynamic peak displacement for different charge mass and scaled distance. Thus, the prediction of this parameter is essential for the comparison of the structural response between two different cases. In their study (Rigby et al., 2019a), a single type of explosive charge was studied (PE4).

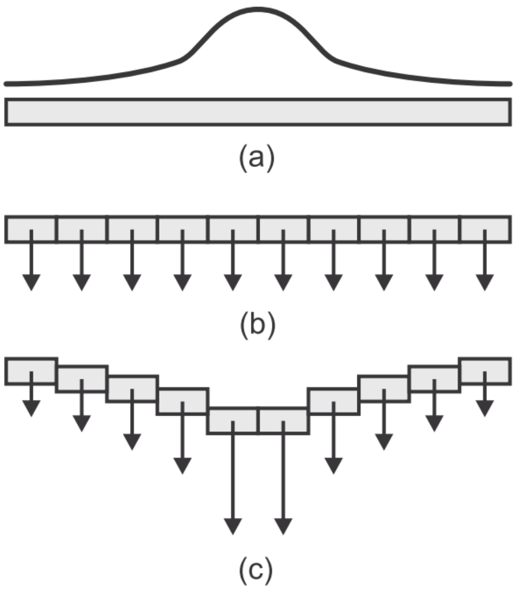

Figure 1 – Nonuniform impulse distribution (a), and modes of deformation related to lower bound (b) and upper bound (c) kinetic energy (Rigby et al., 2019a)

A motivation is raised from the previous information to study and assess the blast loading on plates in the near-field regime, from different explosive types, but with the same mass and standoff distance. The specific impulse distribution has the potential to be different for different explosive types, therefore the main goal of this study is to define the EF for energy equivalent impulse, based on the scaled distance of the charge to the loaded plate face, and the scaled plate dimensions. The main distinction between the current study and previous studies, which dealt with TNT equivalency factors, is that in previous studies the EF was related to blast wave parameters at a single point some distance from the explosive, while in the current study the EF is related to loading distributions which are more closely related to dynamic structural response.

This paper focuses on the derivation and assessment of the TNT EF of three explosives: C4, COMP-B, and ANFO. It is based on numerical hydro-code simulations and uses a common scaling theory. The EF is calculated for each explosive and the results are presented in their scaled form. The paper is outlined as follows: The methodology is explained in the following section, after which the numerical model is presented. The model is validated and verified, and it is used for a parametric study for the assessment of the impulse magnitude and distribution along the radius of a circular plate, for various scaled distances from the target and scaled target sizes. Reference scaled data for TNT explosives is generated from the numerical simulation. The results for C4, COMP-B, and ANFO are scaled and analyzed using the scaling laws to find the equivalent TNT charge which yields the same upper bound kinetic energy that constitutes a representative measure of the dynamic structural response.

2. Methodology

The case considered in the current study refers to the detonation of a spherical charge (initiated at its center) close to a circular thin plate, as illustrated in Figure 2. The charge mass is W, the closest distance from the charge center to the target is R, the target radius is a, and the coordinate along the target radius is $0 \le r \le a$. The coordinate

r corresponds to an angle of θ = arctan(r/R) between the axisymmetric axis and a line connecting the charge center and a point located at coordinate r along the radial direction of the target. The following definitions can be made: The scaled distance between the charge center and the target is $Z = R/W^{1/3}$, and the scaled target radius is $z = a/W^{1/3}$. Note that clearing effects are not considered in the current study.

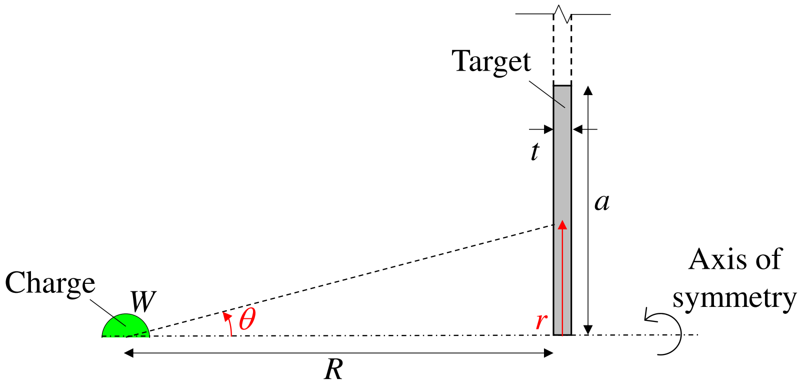

Figure 2 – Layout of the case considered in the current study (axisymmetric view)

As mentioned in the introduction section, the dominant parameter that should be compared between two loading cases to get the same peak displacements is the upper bound kinetic energy of the structure $E_{k,u}$ (Rigby et al., 2019a) that reads:

$$E_{k,u} = \frac{1}{2\rho t}\int_A i^2\left(R,x,y\right)dA \quad (1)$$

where ρ is the density, t is the thickness, i is the nonuniform specific impulse (per unit area), A is the structure surface area exposed to the blast load, and (x, y) are Cartesian coordinates on the target plate, where the origin is the target center. Eq. (1) shows that the impulse distribution over the plate surface is a dominant parameter affecting the kinetic energy. Note that overpressure does not appear in Eq. (1). Due to the high intensity and short duration of the blast load compared to the period of vibrations of the structure, the loading condition is considered impulsive, and the impulse is the only parameter that affects the structural response. In the current study, the structure is a thin circular plate, and for that case, Eq. (1) can be rewritten in polar coordinates:

$$E_{k,u} = \frac{\pi}{\rho t}\int_{r=0}^{r=a} i^2\left(R,r\right)rdr \quad (2)$$

where $i(R,r)$ is the impulse along the radial direction, measured from the circular plate center (see Figure 2). The prediction of the blast load parameters follows the Hopkinson-Cranz scaling laws (Baker, 1973; Cooper, 1996), which are based on Buckingham π theorem. According to the scaling laws, the scaled impulse ($i/W^{1/3}$) is a function of the scaled distance Z. Since the main goal of the current study is to assess the upper bound kinetic energy, it must be scaled as well. Therefore, we present a scaled form of the upper bound kinetic energy which includes the scaled plate parameters (density, thickness, and radius) and the blast parameters (impulse and distance).

The EF for the structural response should be clearly defined. Since the upper bound kinetic energy depends on the scaled distance Z and the target size (defined by the angle of incidence θ, or by the scaled plate radius z), the definition of the equivalent TNT mass is as follows: The equivalent TNT mass is the mass of the examined explosive multiplied by EF, such that it would yield the same upper bound kinetic energy (and hence energy equivalent uniform impulsive load) for a TNT charge located at the same absolute distance from the plate, and for the same plate absolute dimensions.

The numerical model shown in Section 3 provides the impulse and its spatial distribution which is then used to calculate the upper bound kinetic energy. Thus, the numerical model has to be first validated with available experimental results. After its validation, the impulse distributions for various cases are used to calculate the upper bound kinetic energy in each case. The results for the upper bound kinetic energy for various plate sizes, standoff distances, and charge masses are first produced for TNT. Next, the data for TNT is taken as a reference data, to which the results of the other explosives are compared, to find their EF.

3. Numerical modeling

3.1 Geometry and materials

The numerical models are solved in Ansys Autodyn hydro-code (Ansys, 2016). A typical numerical 2D axisymmetric model is shown in Figure 3, for 50 g TNT located 200 mm from the target. The model includes a 400x400 mm^2 Eulerian mesh. The mesh is filled with air and spherical explosive charge (in the axisymmetric model, the spherical charge is represented by a semi-circle shape with its center located along the axisymmetric axis). The detonation point is assumed to be located at the charge center. The target is modeled as a rigid reflected boundary condition along the right vertical boundary, with the implicit assumption that no fluid-structure softening occurs (congruent with the impulsive nature of the loading). The other boundaries (excluding the axisymmetric axis) are modeled with “flow-out” boundary conditions, which allow the detonation products and pressures to vent from the model without any reflections. Numerical gauges are places with intervals of 5 mm along the target radius, to measure the reflected overpressure histories and thus determine specific impulse.

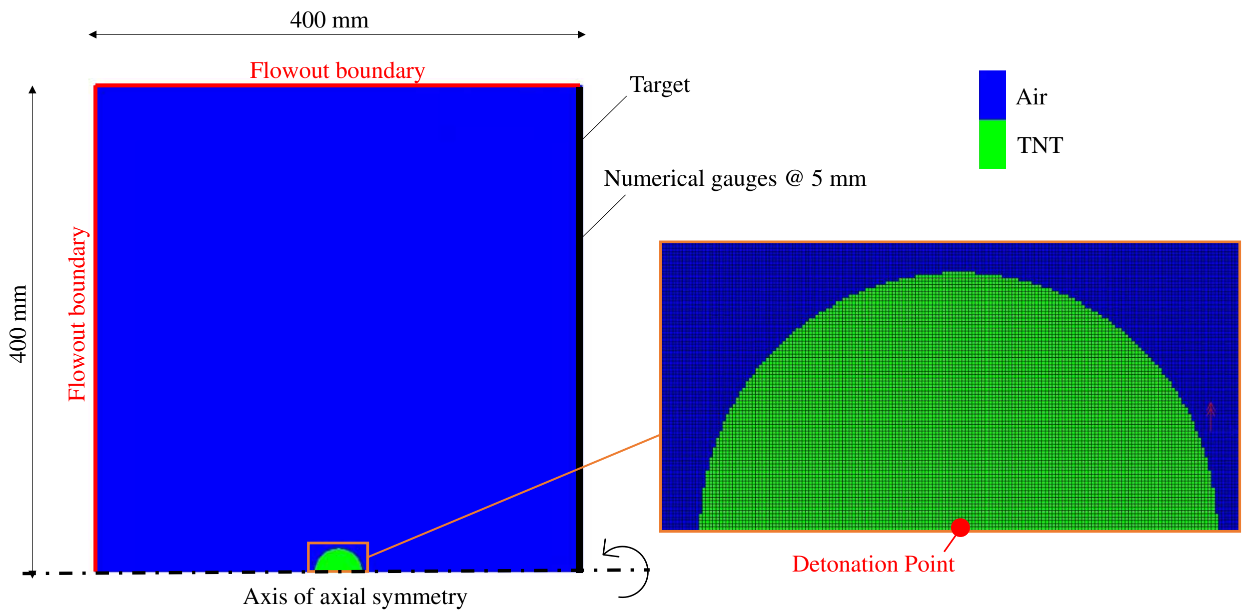

Figure 3 – Typical axisymmetric numerical model

156 The air is modeled with an ideal gas equation of state (EOS) as follows:

$$p = (\gamma - 1)\rho e \tag{3}$$

157 where p is the pressure, $\gamma = 1.4$ is the heat capacity ratio, ρ is the density, and e is the internal energy per unit
158 mass. Initially, the air is assumed to be in standard conditions with a density of $\rho = 1.225$ kg/m^3 and a pressure
159 of $p = 101.332$ kPa. The corresponding internal energy per unit mass is $e = 0.206$ MJ/kg.
160 The explosives are modeled by the Jones-Wilkins-Lee (JWL) EOS (Ansys, 2016; Lee et al., 1968) as shown in
161 Eq. (4):

$$p = A_1\left(1 - \frac{w\rho}{R_1\rho_0}\right)e^{-R_1\frac{\rho_0}{\rho}} + A_2\left(1 - \frac{w\rho}{R_2\rho_0}\right)e^{-R_2\frac{\rho_0}{\rho}} + w\rho e \tag{4}$$

162 where ρ_0 is a reference density. A_1, A_2, R_1, R_2, and w are constants. The detonation velocity, D, and the Chapman-
163 Jouguet pressure, P_{CJ}, are also considered in Autodyn for the detonation process. Four types of explosives are
164 considered in the current study and their well-known JWL parameters are given in Table 1.

Table 1 – JWL EOS parameters for the examined explosives

Explosive	ρ_0 (g/cm^3)	A_1 (kPa)	A_2 (kPa)	R_1	R_2	w	e (MJ/kg)	D (m/s)	P_{CJ} (GPa)
TNT (Dobratz, 1985)	1.63	$3.712 \cdot 10^8$	$3.231 \cdot 10^6$	4.15	0.95	0.30	4.294	6930	21.0
ANFO (Davis and Hill, 2002)	0.93	$4.946 \cdot 10^7$	$1.891 \cdot 10^6$	3.91	1.12	0.33	2.668	4160	5.15
C4 (Dobratz, 1985)	1.60	$6.098 \cdot 10^8$	$1.295 \cdot 10^7$	4.50	1.40	0.25	5.621	8193	28
COMP-B (Dobratz, 1985)	1.72	$5.242 \cdot 10^8$	$7.678 \cdot 10^6$	4.20	1.10	0.34	4.950	7980	29.5

3.2 Convergence study and validation

Since a close-in detonation is modeled, the element size may be critical to achieving sufficient accuracy of the results, and a mesh sensitivity analysis is therefore performed. The element size determined for a converged solution is 0.25 mm, which corresponds to 2.56 million elements in the model. Figure 4 presents an example of the difference between two simulations with two different meshes for 50 g TNT charge located at 50 mm from the target. Results are presented for element sizes of 0.25 mm and 0.5 mm, which includes 640,000 elements. Overall, there is a good agreement between the two cases, with some deviation concentrated in $r \rightarrow 0$ and a maximum difference of approximately 6% between the two cases. In view of the balance between accuracy and computational effort, an element size of 0.25 mm was used to perform a parametric study. It should be noted that for smaller mesh sizes the differences were negligible. A simulation with an element size of 0.25 mm required about 12 hours run time in a standard Intel i7 desktop with 16 GB RAM.

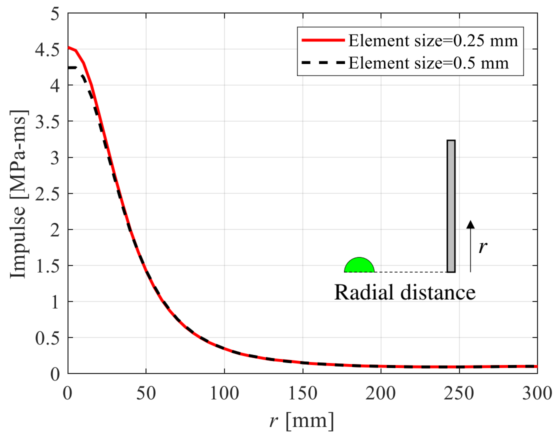

Figure 4 – Mesh sensitivity analysis for 50 g TNT located at 50 mm from the target

3.3 Validation

The numerical results are first validated by comparisons with experimental data. The experimental study of (Rigby et al., 2018, 2019a) in which 100 g spherical PE4 charges were detonated close to large, nominally rigid, circular target plates are used. In these tests, Hopkinson pressure bars were used to measure the reflected overpressure acting on the target along the radial direction. The present modeling uses the JWL parameters of C4 for the PE4 charge as the PE4 explosive is nominally identical to C4 (Rigby et al., 2019a). The impulse was calculated by numerically integrating the overpressure-time history measurements at each gauge with respect to time. Figure 5 shows the peak impulse along the radial direction (which is the vertical direction in the axisymmetric numerical model shown in Figure 3) and compares the numerical results with the experimental ones. The numerical results are within the scatter of the experimental data, and a good agreement is observed.

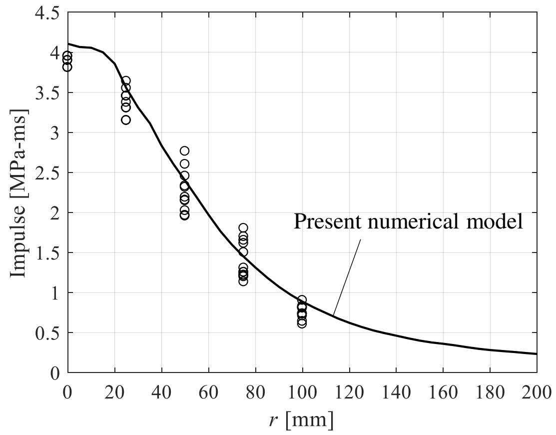

Figure 5 – Validation with experimental data from (Rigby et al., 2019b) for 100 g PE4 located 80 mm from the target

Further validation of the numerical model is achieved by comparing its results to the empirical diagrams given in UFC 3-340-02 (USACE, 2008) for TNT charges. In UFC 3-340-02, the scaled impulse is given as a function of the angle θ. The comparison refers to two cases with scaled distances of Z = 0.198 m/kg$^{1/3}$ and Z = 0.784 m/kg$^{1/3}$. The scaled impulse as a function of the angle of incidence for each case is presented in Figure 6. The numerical results are in good agreement with the TNT-standard empirical data provided in UFC 3-340-02.

The above findings demonstrate the validation and verification of the numerical model. The model is used in the next section for a parametric study to obtain the impulse distribution, which serves as an input parameter for calculating the target kinetic energy for various cases.

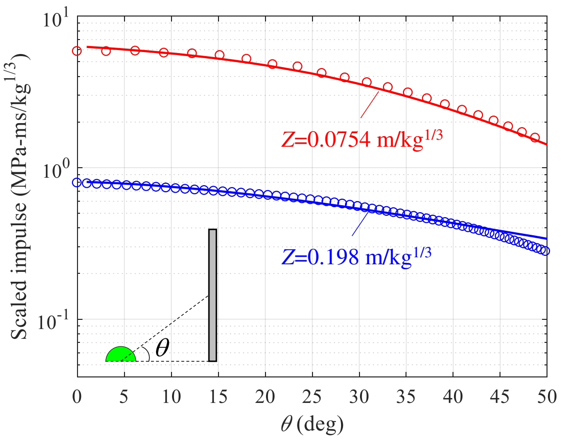

Figure 6 – Comparison with data from the UFC 3-340-02 (USACE, 2008) (solid line: UFC 3-340-02, circle markers: numerical model)

4. Parametric study

4.1 Simulation plan

The numerical model is used to perform a parametric study. Firstly, a set of numerical calculations are performed to establish reference data for TNT, which is then used as the basis for the EF calculation of each explosive. The simulation plan for TNT is shown in Table 2. The charge mass W varies from 0.308 to 50 g. The distance R in Table 2 is defined as the distance between the charge center and the closest point on the target. The corresponding scaled distance, $Z = R/W^{1/3}$, is calculated and shown in Table 2 as well, and they are in the range $0.136 < Z < 3.700$ m//kg$^{1/3}$. The distances R were chosen such that the absolute distance between the charge center and the left vertical flow-out boundary will be no less than 150 mm to avoid any numerical effects of this boundary on the reflected impulse distribution on the target.

Table 2 – Simulation plan for TNT

W (g)	R (mm)	Z (m/kg$^{1/3}$)
50.000	50.0	0.136
50.000	73.0	0.198
50.000	100.0	0.271
50.000	150.0	0.407
50.000	200.0	0.543
50.000	250.0	0.679
2.000	150.0	1.191
2.000	188.0	1.492
2.000	220.0	1.746
0.579	183.3	2.200
0.579	216.7	2.600
0.579	250.0	3.000
0.416	250.0	3.350
0.308	250.0	3.700

After establishing the reference data for TNT, numerical simulations for ANFO, C4 and COMP-B have been performed, and the simulation plan is shown in **Error! Reference source not found.**. In total, 44 simulations have been performed (14 simulations to achieve the reference data for TNT and 10 simulations for each examined explosives). Note that the reference data for TNT is calculated up to Z = 3.7 m/kg$^{1/3}$, while the data for the examined explosives (ANFO, C4 and COMP-B) is calculated up to Z = 3 m/kg$^{1/3}$. The reason is that the value of the EF at Z = 3 m//kg$^{1/3}$ is expected to be calculated, and in the calculation of the EF, the intersection point with the reference TNT curves may exist in the range of Z > 3 m/kg$^{1/3}$.

Table 3 – Simulation plan for ANFO, C4 and COMP-B

W (g)	R (mm)	Z (m/kg$^{1/3}$)
50.000	50	0.136
50.000	73	0.198
50.000	100	0.271
50.000	150	0.407
50.000	200	0.543
50.000	250	0.679
2.000	150	1.191
2.000	188	1.492
2.000	220	1.746
0.579	250	3.000

4.2 Upper bound kinetic energy calculation

As outlined previously, the results of the upper bound kinetic energy for TNT are taken as reference data for the EF calculations. Because the impulse is given in discrete locations along the target radius, where the numerical gauges were placed, the integral in Eq. (2) is numerically solved using the trapezoid numerical method. For each numerical gauge, $E_{k,u}$ is calculated, assuming that the gauge is located at the edge of a given circular plate (i.e. the target radius a is equal to the radial position of the gauge). To describe more general results which can be used in any parameter combination, a scaled form of Eq. (2) should be introduced. After scaling the impulse i, the target radius a, the coordinate along the target radius r, and the target thickness t, by $W^{1/3}$, the scaled form of Eq. (2) is shown in Eq. (5). The density is not scaled according to the scaling theory.

$$\frac{E_{k,u}}{W}\rho\frac{t}{W^{1/3}}=\pi\int_{z=\frac{r}{W^{1/3}}=0}^{z=\frac{r}{W^{1/3}}=\frac{a}{W^{1/3}}}\frac{i^2}{W^{2/3}}\frac{r}{W^{1/3}}dz=f\left(Z,z\right) \quad (5)$$

$E_{k,u}$ depends on the determined values of the target thickness and density, as shown in Eq. (2). However, for the implementation of the scaled form, any value for the thickness and density of the target can be randomly chosen for the absolute value of $E_{k,u}$ calculated by Eq. (2). Although the absolute value of $E_{k,u}$ is divided by the target density and the thickness (Eq. (2)), in the scaled form $E_{k,u}$ is multiplied again by the same values (Eq. (5)), and therefore, the same scaled value is achieved for any target thickness and density (the upper bound kinetic energy relation is assumed to hold, provided the plates can still be considered thin and deform as a membrane). From all simulations, the results are collected and for a given target defined by a scaled dimension z, or a constant angle of incidence θ, the upper bound kinetic energy is calculated as a function of the scaled distance Z between the charge center and the target loaded face.

The upper bound kinetic energy was calculated and scaled for each explosive type from all simulations. Since $E_{k,u}$ is a function of two variables, the left side of Eq. (5) is represented by a surface, defined by Z and z, for each explosive. An example of the scaled surface for TNT is shown in Figure 7 in 2D contour form. Using the same procedure, the surfaces were produced also for ANFO, C4, and COMP-B.

Figure 8 presents an example of a comparison between the scaled upper bound kinetic energy for a given scaled target radius $z = 0.4$ m/kg$^{1/3}$. Note that a gauge that is placed at a given radial distance is located at a different *scaled* distance along the target radius if a different charge mass is used. Hence, in cases where there was no gauge located at $r = zW^{1/3}$ (where $z = 0.4$ m/kg$^{1/3}$ in this example), linear interpolation was applied to estimate the value at $z = 0.4$ m/kg$^{1/3}$. It can be seen that as the scaled distance Z increases, the energy decreases, as expected. For the same conditions (same plate radius, thickness and density, and same standoff distance between the charge and the plate), C4 yielded the highest value of the upper bound kinetic energy and ANFO yielded the lowest one. Therefore, it is expected that there would be different EF values for each explosive, and there is a motivation to study the variation of the EF with scaled distance and scaled target size.

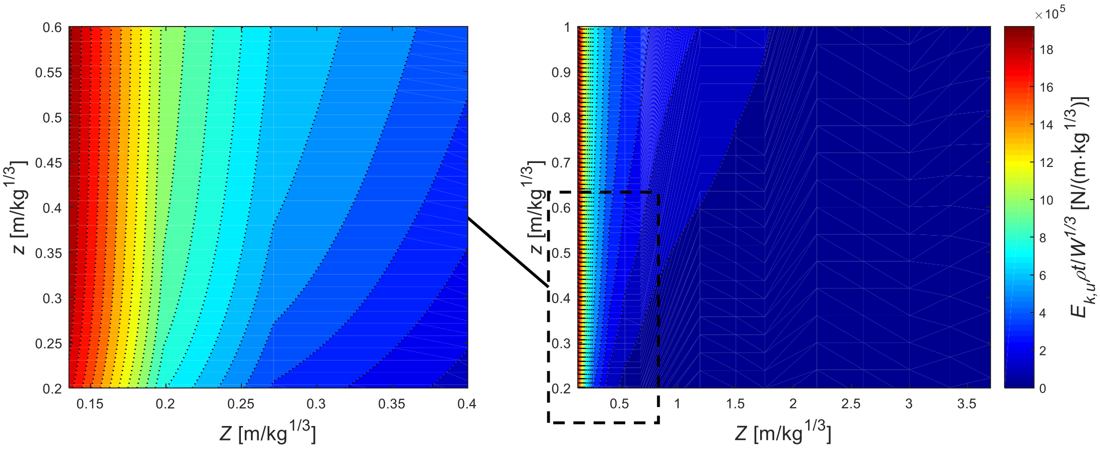

Figure 7 – Example of the scaled upper bound kinetic energy surface for TNT

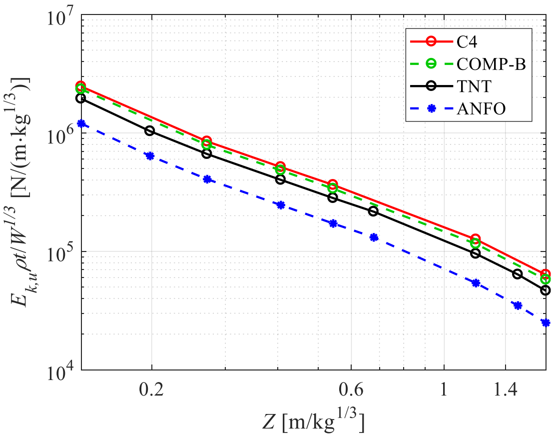

Figure 8 – Example of the scaled upper bound kinetic energy for different explosives and z = 0.4 m/kg$^{1/3}$

5. TNT equivalency factor (EF)

5.1 Calculation approach

The EF for the upper bound kinetic energy (and as a result, for structural response (Rigby et al., 2019a)) was calculated based on blast scaling laws, as follows: It is evident that the upper bound kinetic energy for ANFO, C4, and COMP-B is different than for TNT for the same conditions (same charge mass, absolute distance R, target radius a, and target thickness). Therefore, in order to conserve upper bound kinetic energy (and hence equivalent uniform impulse) when relating the examined explosive to an equivalent mass of TNT, the explosive should be scaled to a different mass of TNT such that its scaled upper bound kinetic energy, scaled distance, and scaled target size would lie on the TNT scaled curves. The results would be considered as the equivalent TNT charge mass to use for the calculation of the EF. When the charge mass is changed, the scaled distance Z and the scaled target radius z are also changed, because they depend on the charge mass. Thus, by changing a point on the scaled surface of an explosive different to TNT by changing the charge mass, all three axes are changed, where the main goal is to transfer this point to the scaled surface of TNT.

The solution is numerically achieved by using the following procedure: Assuming that the scaled surface of the data for TNT is known:

$$\frac{E_{k,u}}{W}\cdot\rho\cdot\frac{t}{W^{1/3}}=f\left(Z,z\right) \tag{6}$$

where f is the surface function for TNT, the equivalent charge mass for the examined explosive is calculated for a specific case by solving the following equation:

$$\frac{E_{k,u}}{W_{eq}}\cdot\rho\cdot\frac{t}{W_{eq}^{\;1/3}}=f\left(Z=\frac{R}{W_{eq}^{\;1/3}},z=\frac{a}{W_{eq}^{\;1/3}}\right) \tag{7}$$

where $E_{k,u}$ is the calculated upper bound kinetic energy for the examined explosive, located at a distance R, for a target defined by the radius a.

The results for the EF are to be presented in scaled form for a given scaled target radius z. First, the scaled values for a given z are found for the examined explosives, for each Z available from the numerical simulations. Eq. (7) is solved using the bisection method. Throughout the numerical procedure, different values of W_{eq} are chosen in an attempt to find the solution. By changing W_{eq}, the scaled target size z and the scaled distance Z are changed. Since the function f of TNT must be used with the "new" z and Z, linear interpolation is applied to produce the data between the known values derived from the numerical simulation. The solution provides the equivalent charge mass W_{eq}, and the resulting EF is the ratio between the calculated equivalent charge mass W_{eq} and the actual charge mass W, i.e. $EF = W_{eq}/W$.

5.2 Results and discussion

The EF is calculated for ANFO, C4, and COMP-B for scaled target sizes of z = 0.2, 0.4, and 0.6 m/kg$^{1/3}$ by applying the suggested procedure over a range of scaled distances. The variation of the EF with the scaled distance Z for the three given values of z is shown in Figure 9, for the three examined explosives. Note that linear interpolation was used in the numerical solution, which is an approximation of the variation between two simulated points on the surface. The results are also presented in Table 4.

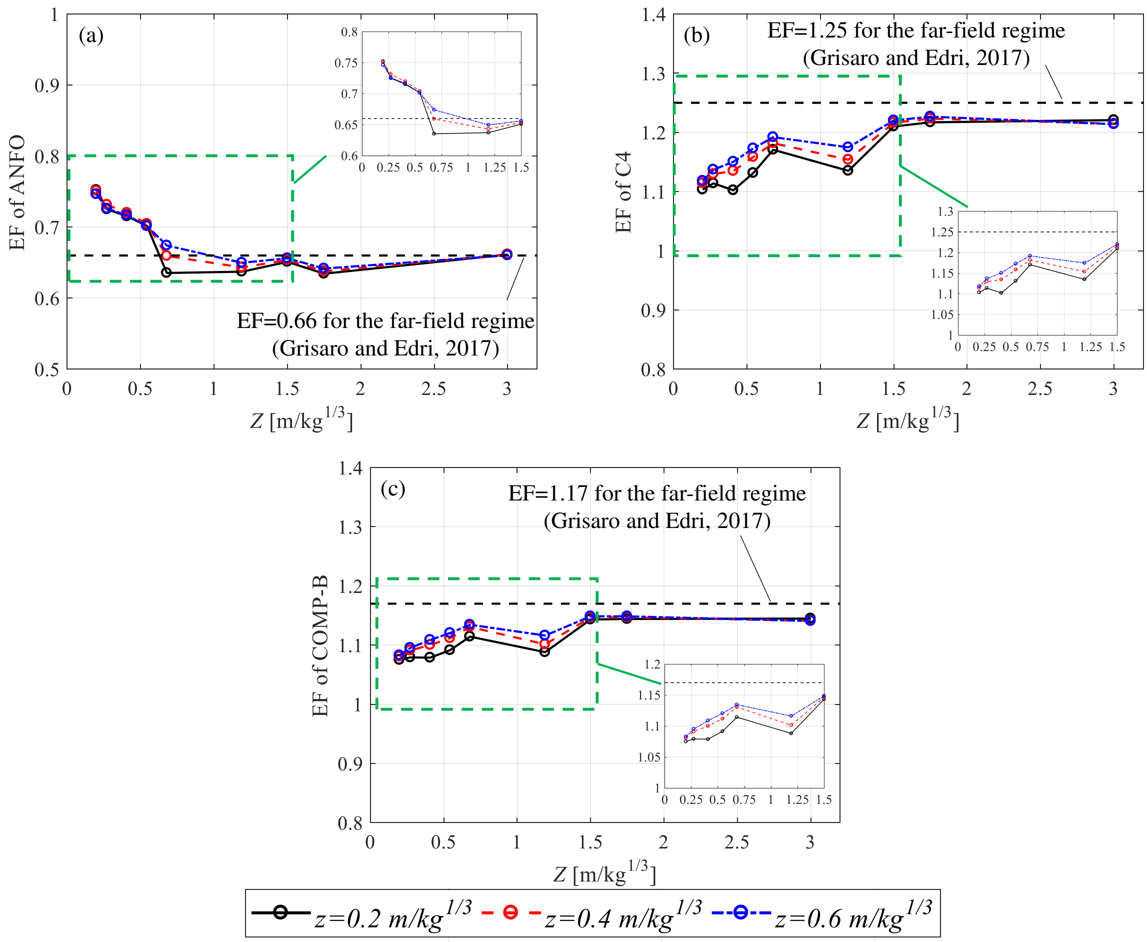

Figure 9 – Calculated EF values for (a) ANFO, (b) C4, and (c) COMP-B

Table 4 – Summary of the TNT equivalency results

Z (m/kg$^{1/3}$)	ANFO			C4			COMP-B		
	z = 0.2 m/kg$^{1/3}$	*z* = 0.4 m/kg$^{1/3}$	*z* = 0.6 m/kg$^{1/3}$	*z* = 0.2 m/kg$^{1/3}$	*z* = 0.4 m/kg$^{1/3}$	*z* = 0.6 m/kg$^{1/3}$	*z* = 0.2 m/kg$^{1/3}$	*z* = 0.4 m/kg$^{1/3}$	*z* = 0.6 m/kg$^{1/3}$
0.198	0.75	0.75	0.75	1.10	1.11	1.12	1.08	1.08	1.08
0.271	0.73	0.73	0.73	1.11	1.13	1.14	1.08	1.09	1.10
0.407	0.72	0.72	0.72	1.10	1.13	1.15	1.08	1.10	1.11
0.543	0.70	0.70	0.70	1.13	1.16	1.17	1.09	1.11	1.12
0.679	0.64	0.66	0.67	1.17	1.18	1.19	1.11	1.13	1.13
1.191	0.64	0.64	0.65	1.14	1.15	1.17	1.09	1.10	1.12
1.492	0.65	0.65	0.66	1.21	1.22	1.22	1.14	1.15	1.15
1.746	0.63	0.64	0.64	1.22	1.22	1.23	1.14	1.15	1.15
3.000	0.66	0.66	0.66	1.22	1.21	1.21	1.14	1.14	1.14

Opposed to the EF values derived in previous studies for the far-field (e.g. Grisaro and Edri, 2017), the calculated EF values for the three examined explosives vary with the scaled distance *Z*, for a given scaled target size *z*. However, the variations are quite moderate with the scaled distance. The EFs for C4 and COMP-B are larger than 1.0, and the EF for ANFO is smaller than 1.0, as expected.

The EFs of ANFO, C4, and COMP-B for far-field explosions were found to be ~0.66, ~1.25, and ~1.17, respectively (Grisaro and Edri, 2017). An interesting observation in this study shows that the EF values for these three explosives converge to these values, as the scaled distance increases (see Figure 9 and Table 4). ANFO converges more closely to the far-field EF values, whereas C4 and COMP-B converge to a value slightly below the (Grisaro and Edri, 2017) values. Within this observation, the EFs of C4 and COMP-B increases as the scaled distance *Z* increases, while it was found that the EF for ANFO decreases as *Z* increases. Our values for the EF for ANFO, C4 and COMP-B in the far-field regime are 0.0%, -2.5% and -2.4% lower than the values obtained by (Grisaro and Edri, 2017), respectively.

By changing the scaled target size *z*, there is a variation between the calculated EF values for C4 and COMP-B, while for ANFO the differences are smaller. In all cases, for the larger *Z*, which is closer to the far-field regime, the differences are negligible. Since specific impulse distribution is affected by explosive type, and different EF values are derived for different scaled distances *Z*, for the largest examined value of *Z* the impulse distribution is more uniform and the effect of target size is therefore less significant. Hence the EF values for increasing *Z* approach those calculated for far-field conditions in a previous study (Grisaro and Edri, 2017), and the effect of the nonuniform distribution is less significant.

6. Summary and conclusions

While TNT equivalency has been previously studied in terms of the blast wave parameters, in the current study, it is studied in terms of the structural response of thin plates under close-in detonations. Accordingly, the equivalency factors are calculated with respect to the upper bound kinetic energy, which was demonstrated to represent a physical measure for the resultant peak dynamic displacement of the plate (Rigby et al., 2019a). The study is based on numerical simulations, which are validated against experimental results and simplified methods. A parametric study is presented, which includes four types of explosives (TNT, ANFO, COMP-B, and C4) placed at various distances from a circular target with various radii. The impulse distribution along the target radial direction, and as a result, the upper bound kinetic energy, are calculated for each simulation and each target size. The TNT equivalency factors are calculated based on analytical considerations and blast wave scaling laws.

The following conclusions are drawn from the current study:

- Unlike the behavior observed in far-field loading conditions, the TNT equivalency factors have been found to vary with the scaled distance in the near-field regime. For the largest scaled distance examined in this study, the EFs tend to converge on the values that have been found in previous studies dealing with far-field explosions. In addition, a change in the scaled target size, z, has a decreasing effect on the variation of the TNT equivalency factors with increasing scaled distance Z.
- For C4 and COMP-B, an increase of the equivalency factors has been observed when increasing the scaled distance Z. However, for ANFO, the opposite trend has been found, and smaller TNT equivalency factors have been obtained for increasing scaled distances.
- The results in the current study have been presented in a scaled form and therefore they can be used for any combination of charge mass, distance from the charge to the target, target size, thickness, and density. As far as the scaled parameters are within the examined scaled limits, no further analyses are required to predict the EF given by the nonuniform impulse distribution acting on the target face.
- The approach presented in the current study includes the following limitations: the analyzed target is relatively thin, and the energy is calculated based on the assumption that there is no variation of the velocity and mass across the target thickness. The clearing effect is ignored. The material constitutive law of the target is linear and any nonlinear effects, accumulation of damage, and potential failure mechanism throughout the response are ignored.
- The results presented in the current paper refer to a spherical charge shape. It is known that charge shape has a significant effect on the blast parameters in the near-field, and therefore, on the structural response, so additional EFs would need to be calculated if the explosive was formed into a different shape. In addition, the charges are detonated at their centroid (i.e. at the center of the sphere) and the point of detonation may affect the impulse distribution in the near-field. However, these features can be easily addressed, and the proposed approach can be augmented to consider their effects on the results.

- The approach presented in the current paper is novel, and it provides important insight regarding the TNT equivalency in the near-field which may be used as a first step when analyzing the blast response of structures under close-in detonations.

References

Adhikary, S. Das, Chandra, L.R., Christian, A., Ong, K.C.G., 2017. Influence of cylindrical charge orientation on the blast response of high strength concrete panels. Eng. Struct. 149, 35–49. https://doi.org/10.1016/J.ENGSTRUCT.2016.04.035

Ansys, 2016. Ansys Autodyn 17.0, Theory manual.

ASCE, 2011. Blast protection of buildings, ASCE/SEI 59-11, American Society of Civil Engineers. Reston, VA.

Baker, W.E., 1973. Explosions in air. University of Texas Press.

Codina, R., Ambrosini, D., 2018. Full-scale testing of leakage of blast waves inside a partially vented room exposed to external air blast loading. Shock Waves 28, 227–241. https://doi.org/10.1007/s00193-017-0733-9

Cooper, P.W., 1996. Explosives engineering. Wiley-VCH.

CSA, 2012. Design and assessment of buildings subjected to blast loads, CSA S850-12, Canadian Standards Association. Mississauga, Ontario, Canada.

Davis, L.L., Hill, L.G., 2002. ANFO Cylinder Tests, in: Shock Compression of Condensed Matter - 2001: 12th Aps Topical Conference. AIP, Atlanta, Georgia, USA. https://doi.org/10.1063/1.1483507

Dobratz, B.., 1985. LLNL explosives handbook : properties of chemical explosives and explosive simulants. Lawrence Livermore National Laboratory, Livermore, CA.

Esparza, E.D., 1986. Blast measurements and equivalency for spherical charges at small scaled distances. Int. J. Impact Eng. 4, 23–40. https://doi.org/10.1016/0734-743X(86)90025-4

Grisaro, H.Y., Edri, I.E., 2017. Numerical investigation of explosive bare charge equivalent weight. Int. J. Prot. Struct. 8, 199–220. https://doi.org/10.1177/2041419617700256

Kingery, C.N., Bulmash, G., 1984. Air blast parameters from TNT spherical air burst and hemispherical surface burst. US Army Ballistic Research Laboratory technical report ARBRL-TR 02555. Maryland, USA.

Lee, E.L., Hornig, H.C., Kury, J.W., 1968. Adiabatic expansion of high explosive detonation products. Report UCRL-50422. University of California, Livermore, CA, USA.

Rigby, S.., Fuller, B., Tyas, A., 2018. Validation of near-field blast loading in LS-Dyna, in: 5th International Conference on Protective Structures (ICPS5). Poznan, Poland, Poland.

Rigby, S., Akintaro, O., Fuller, B., Tyas, A., Curry, R., Langdon, G., Pope, D., 2019a. Predicting the response of plates subjected to near-field explosions using an energy equivalent impulse. Int. J. Impact Eng. 128, 24–36. https://doi.org/10.1016/J.IJIMPENG.2019.01.014

Rigby, S., Tyas, A., Curry, R., Langdon, G., 2019b. Experimental Measurement of Specific Impulse Distribution and Transient Deformation of Plates Subjected to Near-Field Explosive Blasts. Exp. Mech. 59, 163–178.

https://doi.org/10.1007/s11340-018-00438-3

Ritchie, C.B., Packer, J.A., Seica, M. V., Zhao, X.-L., 2018. Behaviour and analysis of concrete-filled rectangular hollow sections subject to blast loading. J. Constr. Steel Res. 147, 340–359. https://doi.org/10.1016/J.JCSR.2018.04.027

Sherkar, P., Whittaker, A., Aref, A., 2014. On the Influence of Charge Shape, Orientation and Point of Detonation on Air-Blast Loadings, in: Structures Congress 2014. American Society of Civil Engineers, Reston, VA, pp. 68–73. https://doi.org/10.1061/9780784413357.007

Shin, J., Whittaker, A., Cormie, D., 2015. Estimating incident and reflected air - blast parameters : updated design charts, in: 16th International Symposium for the Interaction of the Effects of Munitions with Structures (ISIEMS 16). Destin, FL, USA.

USACE, 2008. Unified Facilities Criteria (UFC) - Structures to resist the effects of accidental explosions. UFC 3-340-02, U.S Army Corps of Engineers.

Xiao, W., Andrae, M., Gebbeken, N., 2020. Air Blast TNT Equivalence Concept for Blast-Resistant Design. Int. J. Mech. Sci. 105871. https://doi.org/10.1016/j.ijmecsci.2020.105871

Xiao, W., Andrae, M., Gebbeken, N., 2019. Air blast TNT equivalence factors of high explosive material PETN for bare charges. J. Hazard. Mater. 377, 152–162. https://doi.org/10.1016/j.jhazmat.2019.05.078